LETTERS

Histone arginine methylation regulates pluripotency in the early mouse embryo

Maria-Elena Torres-Padilla[1], David-Emlyn Parfitt[1], Tony Kouzarides[1] & Magdalena Zernicka-Goetz[1]

It has been generally accepted that the mammalian embryo starts its development with all cells identical, and only when inside and outside cells form do differences between cells first emerge. However, recent findings show that cells in the mouse embryo can differ in their developmental fate and potency as early as the four-cell stage[1–4]. These differences depend on the orientation and order of the cleavage divisions that generated them[2,5]. Because epigenetic marks are suggested to be involved in sustaining pluripotency[6,7], we considered that such developmental properties might be achieved through epigenetic mechanisms. Here we show that modification of histone H3, through the methylation of specific arginine residues, is correlated with cell fate and potency. Levels of H3 methylation at specific arginine residues are maximal in four-cell blastomeres that will contribute to the inner cell mass (ICM) and polar trophectoderm and undertake full development when combined together in chimaeras. Arginine methylation of H3 is minimal in cells whose progeny contributes more to the mural trophectoderm and that show compromised development when combined in chimaeras. This suggests that higher levels of H3 arginine methylation predispose blastomeres to contribute to the pluripotent cells of the ICM. We confirm this prediction by overexpressing the H3-specific arginine methyltransferase CARM1 in individual blastomeres and show that this directs their progeny to the ICM and results in a dramatic upregulation of Nanog and Sox2. Thus, our results identify specific histone modifications as the earliest known epigenetic marker contributing to development of ICM and show that manipulation of epigenetic information influences cell fate determination.

To address whether epigenetic differences exist between blastomeres at the four-cell stage, we focused on histone methylation marks related to transcriptional activation[8–10]. Because the divisions of two-cell-stage blastomeres differ in orientation in relation to the animal–vegetal axis of the egg[5,11], the shapes of four-cell embryos vary: blastomeres fill the apices of a tetrahedron when they undergo one equatorial (E) and one meridional (M) division, or they lie on a similar plane when they undergo either two E or two M divisions (Fig. 1a). Although any combination of the temporal sequence of such divisions is possible, sequential M and E divisions are most common (about 80%), but they can occur in either order. We found that whereas embryos that underwent either two E or two M divisions did not show significant variations in the levels of H3 methylation at Arg 26 (H3R26me) between four-cell-stage blastomeres (Fig. 1a, EE and MM embryos; blue bars), tetrahedral embryos showed marked differences in H3R26me levels between their blastomeres (Fig. 1a, EM and ME embryos; red bars). In the latter, the weakest level of H3R26me was generally less than 40% of the cell giving the strongest signal ($P = 0.0002$). Measuring the intensity of DNA staining indicated that the variation of H3R26me levels was not related to differences in the content of DNA resulting from replication (not shown). We confirmed that this variation in H3R26me levels did not result from the confocal scanning of embryos of differing shapes by scanning individual cells of disaggregated embryos, where we found a similar outcome (Supplementary Fig. S1). In addressing whether the methylation of other arginine residues also showed differences between four-cell blastomeres, we found that levels of H3R2me and H3R17me (Supplementary Figs S2 and S3a) varied between blastomeres correlating with embryo morphology in a similar way to H3R26me. This is consistent with Arg 2 and Arg 17 being targets for the same methyltransferase, CARM1, as Arg 26 (refs 12, 13). When we analysed CARM1 distribution in four-cell blastomeres, we found that CARM1 levels varied with the same tendency as those of H3R26me (Supplementary Fig. S4b, c). In contrast, methylation of H4R3, which is the target of a different methyltransferase, protein arginine methyltransferase 1 (PRMT1; refs 14, 15), seemed equivalent between blastomeres regardless of embryo morphology (Fig. 1b). Thus, the differences in the levels of histone arginine methylation in four-cell-stage blastomeres are specific. We also observed that levels of BrUTP incorporation in late four-cell-stage embryos were highest in the blastomeres that were enriched for H3R26me, indicative of elevated levels of global transcription in these cells (Fig. 1c–e). Because H3R26me showed the biggest difference in its distribution between blastomeres (Supplementary Fig. S3b), we concentrated on analysing this modification further.

Because different developmental fate and potential can be ascribed to blastomeres depending on the orientation and the order of division from the two-cell to the four-cell stage in relation to the animal–vegetal axis, we wished to determine whether differences in H3R26me related to patterns of division. To this end we first grouped embryos according to their cleavage patterns to the four-cell stage. When the earlier of the second cleavages is M and the later E (ME embryos), the earlier dividing two-cell blastomere contributes most of its progeny to the embryonic (ICM and adjacent polar trophectoderm) and the later one to the abembryonic part (ICM and mural trophectoderm) of the blastocyst. When the earlier second cleavage is E and the later is M (EM embryos), the earlier blastomere can give rise to either the embryonic or abembryonic part of the blastocyst. By contrast, when second cleavage divisions are of similar orientation (MM or EE), the allocation of blastomere progeny is random. The ME group of embryos thus allowed the identification of individual four-cell blastomeres that have a predictable fate within the blastocyst[5]. Moreover, blastomeres resulting from the E division that inherit the 'vegetal' cytoplasm in ME embryos tend to contribute more to the mural trophectoderm and do not complete development when combined with the same type of 'vegetal' cells in chimaeric embryos[2]. In contrast, chimaeras of blastomeres that arise from early M divisions (with 'animal–vegetal' cytoplasm) could complete development with full success, and chimaeras constructed only from 'animal' blastomeres could also develop although with reduced success.

[1]The Wellcome Trust/Cancer Research UK Gurdon Institute, University of Cambridge, Tennis Court Road, Cambridge CB2 1QN, UK.

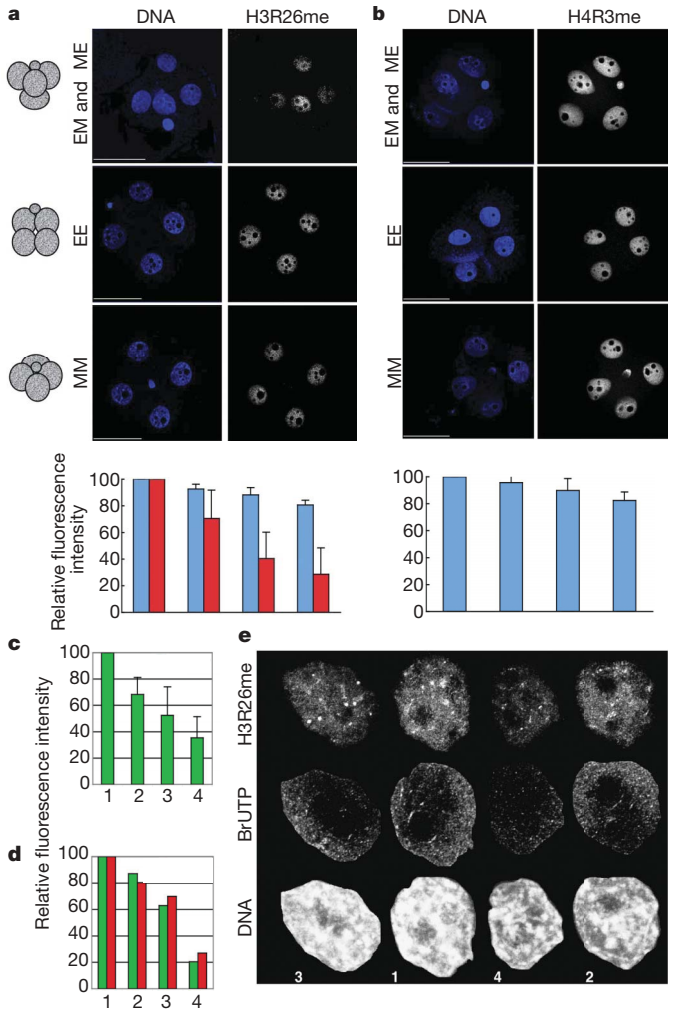

Figure 1 | Levels of H3R26me are different in blastomeres of four-cell-stage embryos and correlate with their spatial arrangement. **a**, Four-cell-stage embryos were stained for H3R26me and grouped according to their shape: tetrahedral (EM and ME), EE (flattened, polar body on one side) or MM (flattened, polar body in the middle). Shown are projections, including all sections, of representative embryos. Fluorescence levels were quantified and normalized against the blastomere showing the highest level, which was set at 100%. Decreasing values of fluorescence were normalized and averaged accordingly ($n = 18$). Each bar represents the relative fluorescence level of each of the four blastomeres: red bars, EM and ME embryos; blue bars, MM or EE embryos. Scale bar, 50 μm. **b**, Differences in histone arginine methylation levels in four-cell-stage blastomeres are specific: only residues that are CARM1 targets, and not PRMT1, show differential distribution. The histogram gives results for embryos of all shapes. **c**, Four-cell-stage blastomeres show different global transcriptional activities. BrUTP incorporation was measured in sections from nuclei of four-cell-stage embryos captured every 0.6 μm ($n = 12$). Projections were used after cropping off the nuclei with the Volocity software to quantify active (nuclear) transcription. Values were normalized as in **a**. **d**, **e**, Global transcription levels correlate with global H3R26me levels. **d**, Quantification of BrUTP incorporation (green) and H3R26me (red) of nuclei of each four-cell blastomere of a representative embryo. **e**, Nuclei shown at the same scale, numbers at the bottom correspond to the blastomere numbers of the graph in **d**. Error bars indicate s.d.

To distinguish the progeny of two-cell-stage blastomeres, we injected one two-cell blastomere at random with rhodamine-dextran and then monitored the second cleavage divisions (Supplementary Fig. S5a). Immunostaining then revealed similar levels of H3R26me in the progeny of both E and M divisions of EM embryos (compare M cells with E cells; $P = 0.112$; Supplementary Fig. S5b, c). In ME embryos, however, the M sister cells had significantly higher levels of H3R26 methylation than both E sisters, with one of the E-derived blastomeres showing significantly less methylation than either of the M-derived blastomeres ($P < 0.0001$; Supplementary Fig. S5b, c). In confirmation of our earlier observations (Fig. 1), EE and MM embryos did not show differences in their relative H3R26me levels. Thus, in ME embryos in which prediction of developmental properties is possible, higher levels of H3R26me are seen in blastomeres expected to contribute more cells to the embryonic part of the blastocyst and lower levels in blastomeres expected to contribute to the abembryonic part.

Given the reported differences in developmental potential of 'animal' and 'vegetal' blastomeres arising from E divisions in ME embryos[2], we next examined whether these cells differed in their H3R26me levels. To this end we randomly injected a two-cell-stage blastomere with rhodamine-dextran as before and then applied green fluorescent beads to the vegetal membranes of the two blastomeres as a second label (Fig. 2a and ref. 2). The rhodamine label allowed us to score the order and the plane of division to the four-cell-stage and the beads served as 'vegetal' markers. We found that in ME embryos, the 'vegetal' blastomere always had significantly lower levels of H3R26me than the 'animal' or 'animal/vegetal' blastomeres ($P < 0.0001$;

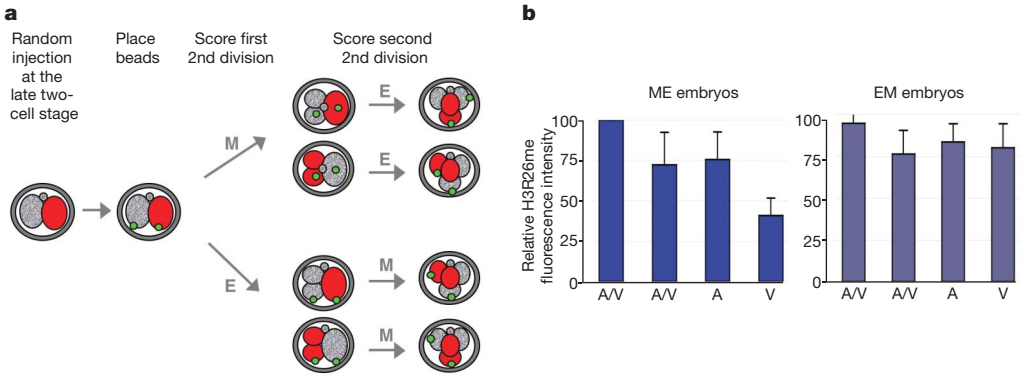

Figure 2 | The 'vegetal' blastomere in ME embryos has the lowest levels of H3R26me. **a**, Design to determine the identity of four-cell-stage blastomeres according to division orientation, order, and blastomere positioning. A two-cell-stage blastomere was microinjected with rhodamine-dextran. We then placed a green fluorescent bead in the 'vegetal' membrane of the two blastomeres. Divisions were scored and embryos were stained for H3R26me at the late four-cell stage. The position of the bead and the presence of rhodamine allowed the identification of the blastomeres as animal/vegetal (A/V, derived from M divisions), or animal or vegetal (A or V, derived from E divisions) in EM ($n = 10$) or ME ($n = 9$) embryos. **b**, The vegetal blastomere of ME embryos shows the lowest levels of H3R26me, whereas the vegetal blastomere of EM embryos shows similar levels to the animal or animal/vegetal blastomeres. H3R26me levels were quantified as in Fig. 1. Because there are two A/V blastomeres after one M division there are two columns labelled A/V. Error bars indicate s.d.

Fig. 2b). In contrast, in EM embryos the 'animal' and 'vegetal' blastomeres from the E division had equivalent levels of H3R26me (Fig. 2b). Taken together, our results indicate that more extensive H3 arginine methylation in M blastomeres of ME embryos is correlated with their greater contribution to the embryonic part of the blastocyst. In contrast, blastomeres having the lowest levels of H3 arginine methylation (that is, 'vegetal' blastomeres) are those predicted to contribute mainly to the abembryonic part.

Because levels of methylation at Arg 2, Arg 17 and Arg 26 varied similarly and because these three residues are the specific targets of CARM1/PRMT4, which is expressed maternally in mouse embryos (Supplementary Figs S4 and S6), we wondered whether CARM1

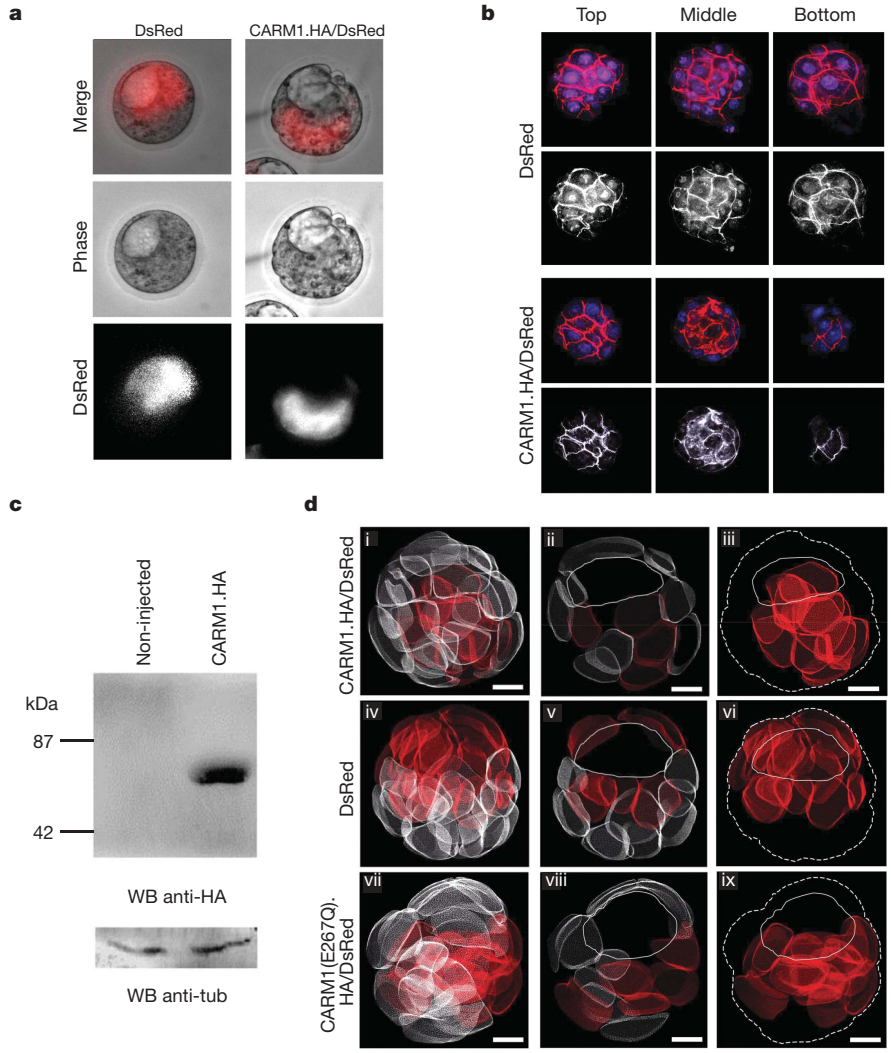

e

	Total no. of cells	No. of red cells (% of all cells)	No. of inner (% all cells)	Inner positive (% of inner)	Red that are inner (%)	No. of outer (% of all cells)	Outer positive (% of outer)	Red that are outer (%)	No. of embryos analysed
CARM1	27.5 ± 4.62	41.17 ± 9.32	37.36 ± 9.11	88.53 ± 13.73	80.24 ± 11.56	62.64 ± 9.25	12.76 ± 7.35	19.76 ± 11.56	10
CARM1(E267Q)	32.8 ± 2.62	47.84 ± 5.55	35.71 ± 2.42	54.86 ± 12.86	41.39 ± 7.32	64.29 ± 2.42	43.59 ± 7.11	58.61 ± 7.32	10
DsRed control	30.30 ± 3.30	45.31 ± 3.8	28.10 ± 6.90	66.9 ± 10.22	41.31 ± 10.26	71.9 ± 6.90	37.1 ± 7.37	58.7 ± 10.26	10
					$P<0.0001$			$P<0.0001$	

Figure 3 | CARM1 overexpression in a two-cell blastomere results in the contribution of that cell predominantly to the ICM. A late two-cell-stage blastomere was injected with mRNA for DsRed alone (control) or in combination with mRNA for CARM1.HA (HA stands for haemagglutinin). This resulted in CARM1 overexpression from the mid-four-cell stage because CARM1.HA/DsRed expression starts 6–8 h after injection (not shown). Embryos were cultured until the blastocyst stage and observed under fluorescence microscopy. DsRed was used as a lineage tracer. **a**, Representative embryos derived from DsRed only ($n = 17$) or DsRed/CARM1.HA-overexpression experiments ($n = 35$). **b**, Blastocysts were stained with phalloidin–Texas red and TOTO-3 (to reveal cell membranes and DNA, respectively) and analysed under confocal microscopy. Representative top, middle and bottom sections are shown. DNA is in blue; phalloidin (red) can be distinguished from DsRed because the latter is exclusively cytoplasmic. The red channel is shown as a greyscale. The progeny of the CARM1-overexpressing blastomere is predominantly within the inner cells of the blastocyst. **c**, Overexpression of CARM1 was verified by western blot (WB) analysis in zygotes injected with mRNA for CARM1.HA/DsRed. **d**, Representative three-dimensional reconstructions of blastocysts in which mRNA for CARM1.HA/DsRed (i), Ds/Red only (iv) or CARM1(E267Q).HA/DsRed (vii) was microinjected at the two-cell stage. Blastocysts were stained as in **b**. Confocal *z*-stacks were taken at 1-μm intervals. IMARIS software was used to outline cell membranes to create three-dimensional models of all cells of the embryo. Cells were then scored according to their position: cells completely surrounded by others are denoted as inner, those with an outer surface as outer. Cells were scored as either positive or negative for DsRed. Progeny of injected blastomere is shown in red. A middle slice is shown in ii, v and viii, where the cavity is depicted with a line. In iii, vi and ix, only the progeny of the injected blastomere is shown; the contour of the embryo is indicated by a dashed line and the position of the cavity by a solid line. Scale bar, 10 μm. **e**, Analysis of the distribution of the progeny of CARM1- and DsRed-overexpressing blastomere at the blastocyst stage. Results are means ± s.d.

might have a function in directing developmental fate and potency. To test this, we injected CARM1 mRNA into single late two-cell-stage blastomeres aiming to elevate levels of arginine methylation in H3 in the progeny of these cells from the mid-four-cell stage. We followed the effect on cell fate by co-injecting mRNA for DsRed as a lineage tracer (Fig. 3a, b). Strikingly, the labelled clone was located in the embryonic part of the blastocyst in 31 out of 35 embryos (89%), and in no embryos were labelled cells found exclusively in the abembryonic part. We randomly selected ten of these embryos for reconstruction in three dimensions to locate every cell and determine to which lineage (ICM or trophectoderm) labelled cells had contributed. This showed that the ICM comprised 37% of all cells at this stage and that, on average, 88.5% of ICM cells were derived from the blastomere in which CARM1 had been overexpressed (Fig. 3d, e, and Supplementary Table S1). Interestingly, in half of the embryos, all of the ICM comprised the exclusive progeny of the CARM1-overexpressing blastomere. By contrast, even though most (63%) of the blastocyst cells are outer cells, the proportion of outer cells derived from the CARM1-overexpressing blastomere was only 12% (Fig. 3e, and Supplementary Table S1). This was in contrast with control embryos, injected with mRNA for DsRed only, in which we found that 41% and 59% of cells labelled with the lineage tracer were inner and outer cells, respectively ($P < 0.0001$; Fig. 3e, and Supplementary Table S2). We therefore conclude that forced overexpression of CARM1 in a two-cell blastomere leads that cell to contribute predominantly (if not exclusively) to the ICM. To establish whether the methyltransferase activity of CARM1 was required for this effect, we injected mRNA for CARM1 containing a point mutation (E267Q) and devoid of catalytic activity[16] into single two-cell blastomeres as above. We found that the progeny of the labelled cells could contribute to both embryonic and abembryonic regions of the blastocyst. The distribution of the progeny of the blastomere injected with CARM1(E267Q) was similar to that of the DsRed control (Fig. 3d, e, and Supplementary Table S3). The progeny of the CARM1-overexpressing blastomere showed increased levels of H3R26me, whereas blastomeres overexpressing CARM1(E267Q) did not (Fig. 4a, b). Hence, the ability of CARM1 to direct the progeny of a blastomere towards the ICM is strictly dependent on its methyltransferase activity.

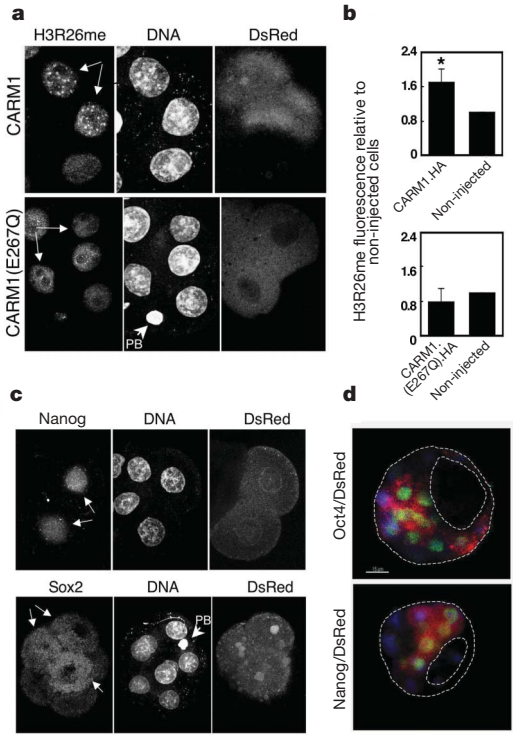

Figure 4 | Overexpression of CARM1 results in elevated levels of arginine methylation and upregulation of Nanog and Sox2. **a**, A two-cell-stage blastomere was injected with mRNA for CARM1.HA/DsRed. Embryos were cultured to the eight-cell stage and stained for H3R26me. Shown are three nuclei of cells from a representative embryo. The progeny of the injected blastomere is indicated by arrows (note the presence of DsRed). For overexpression of the CARM1(E267Q). HA mutant, five cells from the same embryo are shown ($n = 6$). PB, polar body. **b**, Quantification of H3R26me levels in cells overexpressing CARM1 were normalized against those of non-injected cells within the same embryo (asterisk, $P = 0.0006$; $n = 14$). Bottom: data derived from overexpression of CARM1(E267Q).HA. Error bars indicate s.d. **c**, Embryos were injected as in **a** and stained with an anti-Nanog ($n = 5$) or an anti-Sox2 ($n = 11$) antibody between the six-cell and the eight-cell stage. For Nanog, four nuclei from the same embryo, two of them deriving from the CARM1-overexpressing blastomere, are shown (white arrows; note the presence of DsRed). Nanog is detectable only in the blastomeres deriving from the two-cell-stage blastomere injected with CARM1 mRNA. For Sox2, a representative embryo is shown. Note that Sox2 is mainly cytoplasmic at this stage[18]. We were unable to address CARM1 function by the converse experiment by RNA-mediated interference because the protein is provided maternally and its mRNA is rapidly downregulated after fertilization. However, treatment of zygotes with specific arginine methyltransferase inhibitors[25] showed that decreasing the level of histone arginine methylation impaired development (Supplementary Fig. S8). **d**, The progeny of a CARM1-overexpressing blastomere expresses ICM markers in the blastocyst. Blastocysts were stained for Oct4/Pou5f1 ($n = 7$) or Nanog ($n = 3$; green). The presence of DsRed indicates the progeny of the injected blastomere. DNA is shown in blue.

We next assessed expression levels of transcription factors known to influence the development of ICM cells. We found that overexpression of CARM1 led to an early and marked upregulation of Nanog in the injected blastomeres, suggesting that the Nanog promoter is regulated by arginine methylation (Fig. 4c). In contrast, Cdx2, a trophectoderm marker, showed no induction after overexpression of CARM1 (not shown). We also detected increased levels of Sox2 in the progeny of the CARM1-injected blastomere (Fig. 4c). However, Oct4/Pou5f1 showed variable levels of expression in non-injected blastomeres as well as in cells overexpressing CARM1 (Supplementary Fig. S7). Note that, in contrast with Nanog, both Oct4/Pou5f1 and Sox2 were also present in the non-injected blastomeres, reflecting an earlier expression and/or their maternal inheritance[17,18]. The co-expression by the blastocyst stage of the ICM markers Oct4/Pou5f1 and Nanog in the progeny of the CARM1-overexpressing blastomere is consistent with the observed change in cell fate (Fig. 4d). Hence, by manipulating epigenetic information through the overexpression of a histone modifier it is possible to direct cells towards the ICM.

Our findings, in control experiments, that either of the two-cell blastomeres normally contributes its progeny to both inner and outer cells of the blastocyst are in accordance with our earlier findings[1,2,4,5]. However, they contrast with a report that shows that as a consequence of differential Cdx2 levels between two-cell blastomeres, one blastomere contributes exclusively to outer cells, which normally express Cdx2 (ref. 19). Unlike those authors we do not observe expression of Cdx2 at the two-cell stage.

Our study demonstrates that epigenetic differences develop between blastomeres by the four-cell stage. We cannot exclude the possibility that CARM1 mediates some of its effects through targets other than histone H3. However, the differential cellular levels of H3 methylation within four-cell blastomeres can account for their different cell fates and potencies[1,4,5]. Cells with more extensive H3 arginine methylation are destined to contribute pluripotent progeny to the blastocyst. These cells show increased levels of transcription, including the expression of a select set of genes responsible for maintaining pluripotency such as Nanog and Sox2 (refs 18, 20, 21). An enrichment in modifications characteristic of euchromatin may have additional effects on the chromatin to generate an 'open' configuration that could sustain pluripotency in the embryo, as has been suggested for ES cells[22]. Indeed, the relative importance of potential changes in chromatin structure in relation to cell plasticity demands further study.

METHODS

Embryos were collected from F_1 crosses (C57BL/6XCBA/H). To monitor the division from the two-cell stage, one blastomere was microinjected randomly with dextran-tetramethylrhodamine (3 kDa; Molecular Probes). Green fluorescent beads were placed in the membrane of blastomeres with the use of a Piezo driller. Embryos were observed every 20 min to determine the plane and order of division[5]. Immunostaining and BrUTP labelling were performed as described[23]. Anti-H3 asymmetric-dimethyl-Arg 2, anti-H3 dimethyl-Arg 17, anti-H3 dimethyl-Arg 26 and anti-H4 symmetric-dimethyl-Arg 3 antibodies were from Abcam (Supplementary Fig. S9); anti-Oct4 was from R&D Systems; and anti-Nanog and anti-Sox2 were from Santa Cruz. For analysis of four-cell embryos, confocal sections were taken every 0.8 μm through the whole embryo and the fluorescence signal was measured in projections with the Volocity software (Improvision). For three-dimensional reconstructions, blastocysts were stained with phalloidin–Texas red and TOTO-3. Confocal sections were captured every 1 μm and processed with IMARIS (Bitplane) and 3DVirtual Embryo software[24].

Received 9 August; accepted 17 November 2006.

1. Piotrowska, K., Wianny, F., Pedersen, R. A. & Zernicka-Goetz, M. Blastomeres arising from the first cleavage division have distinguishable fates in normal mouse development. *Development* **128,** 3739–3748 (2001).
2. Piotrowska-Nitsche, K., Perea-Gomez, A., Haraguchi, S. & Zernicka-Goetz, M. Four-cell stage mouse blastomeres have different developmental properties. *Development* **132,** 479–490 (2005).
3. Gardner, R. L. Specification of embryonic axes begins before cleavage in normal mouse development. *Development* **128,** 839–847 (2001).
4. Fujimori, T., Kurotaki, Y., Miyazaki, J. & Nabeshima, Y. Analysis of cell lineage in two- and four-cell mouse embryos. *Development* **130,** 5113–5122 (2003).
5. Piotrowska-Nitsche, K. & Zernicka-Goetz, M. Spatial arrangement of individual 4-cell stage blastomeres and the order in which they are generated correlate with blastocyst pattern in the mouse embryo. *Mech. Dev.* **122,** 487–500 (2005).
6. Li, E. Chromatin modification and epigenetic reprogramming in mammalian development. *Nature Rev. Genet.* **3,** 662–673 (2002).
7. Morgan, H. D., Santos, F., Green, K., Dean, W. & Reik, W. Epigenetic reprogramming in mammals. *Hum. Mol. Genet.* **14** (Spec. Iss. 1), R47–R58 (2005).
8. Chen, D. *et al.* Regulation of transcription by a protein methyltransferase. *Science* **284,** 2174–2177 (1999).
9. Ma, H. *et al.* Hormone-dependent, CARM1-directed, arginine-specific methylation of histone H3 on a steroid-regulated promoter. *Curr. Biol.* **11,** 1981–1985 (2001).
10. Bauer, U. M., Daujat, S., Nielsen, S. J., Nightingale, K. & Kouzarides, T. Methylation at arginine 17 of histone H3 is linked to gene activation. *EMBO Rep.* **3,** 39–44 (2002).
11. Gardner, R. L. Experimental analysis of second cleavage in the mouse. *Hum. Reprod.* **17,** 3178–3189 (2002).
12. Bannister, A. J. & Kouzarides, T. Reversing histone methylation. *Nature* **436,** 1103–1106 (2005).
13. Schurter, B. T. *et al.* Methylation of histone H3 by coactivator-associated arginine methyltransferase 1. *Biochemistry* **40,** 5747–5756 (2001).
14. Wang, H. *et al.* Methylation of histone H4 at arginine 3 facilitating transcriptional activation by nuclear hormone receptor. *Science* **293,** 853–857 (2001).
15. Strahl, B. D. *et al.* Methylation of histone H4 at arginine 3 occurs *in vivo* and is mediated by the nuclear receptor coactivator PRMT1. *Curr. Biol.* **11,** 996–1000 (2001).
16. Lee, Y. H., Koh, S. S., Zhang, X., Cheng, X. & Stallcup, M. R. Synergy among nuclear receptor coactivators: selective requirement for protein methyltransferase and acetyltransferase activities. *Mol. Cell. Biol.* **22,** 3621–3632 (2002).
17. Scholer, H. R., Hatzopoulos, A. K., Balling, R., Suzuki, N. & Gruss, P. A family of octamer-specific proteins present during mouse embryogenesis: evidence for germline-specific expression of an Oct factor. *EMBO J.* **8,** 2543–2550 (1989).
18. Avilion, A. A. *et al.* Multipotent cell lineages in early mouse development depend on SOX2 function. *Genes Dev.* **17,** 126–140 (2003).
19. Deb, K., Sivaguru, M., Yong, H. Y. & Roberts, R. M. Cdx2 gene expression and trophectoderm lineage specification in mouse embryos. *Science* **311,** 992–996 (2006).
20. Mitsui, K. *et al.* The homeoprotein Nanog is required for maintenance of pluripotency in mouse epiblast and ES cells. *Cell* **113,** 631–642 (2003).
21. Chambers, I. *et al.* Functional expression cloning of Nanog, a pluripotency sustaining factor in embryonic stem cells. *Cell* **113,** 643–655 (2003).
22. Meshorer, E. *et al.* Hyperdynamic plasticity of chromatin proteins in pluripotent embryonic stem cells. *Dev. Cell* **10,** 105–116 (2006).
23. Torres-Padilla, M. E. & Zernicka-Goetz, M. Role of TIF1α as a modulator of embryonic transcription in the mouse zygote. *J. Cell Biol.* **174,** 329–338 (2006).
24. Tassy, O., Daian, F., Hudson, C., Bertrand, V. & Lemaire, P. A quantitative approach to the study of cell shapes and interactions during early chordate embryogenesis. *Curr. Biol.* **16,** 345–358 (2006).
25. Cheng, D. *et al.* Small molecule regulators of protein arginine methyltransferases. *J. Biol. Chem.* **279,** 23892–23899 (2004).

Supplementary Information is linked to the online version of the paper at www.nature.com/nature.

Acknowledgements We thank P. Greda for bead labelling, C. Lee for assistance, D. Glover for comments on the manuscript, M. Stallcup for the CARM1 expression vectors, and M. Bedford for providing the *Carm1*$^{-/-}$ MEFs and the PRMT inhibitor. M.-E.T.-P. is an EMBO long-term fellow. We are grateful to the Wellcome Trust Senior Fellowship to M.Z.-G., which supported this work.

Author Information Reprints and permissions information is available at www.nature.com/reprints. The authors declare no competing financial interests. Correspondence and requests for materials should be addressed to M.Z.-G. (mzg@mole.bio.cam.ac.uk).